Modeling Efficacy of Prescribed Burning in Reducing Wildfires in California

Michael Xiao

ABSTRACT

Prescribed burning is a fire management technique used to reduce wildfire risks. The current scheme for prescribed burning in California is sub-optimal, with wildfires continuing to increase despite management efforts. This study examines the effectiveness of prescribed burning in reducing wildfire occurrences and scale in California. We collected gridded data on prescribed burning, wildfires, along with 15 other covariates that influence wildfire trends and constructed a generalized additive model of these factors on wildfire ignition probability and wildfire scale. The result showed a decrease in wildfire ignition probability with increasing levels of prescribed burning from 2016 to 2019, but the effect is only significant if more than 20% of the grid is burned. In relation to wildfire ignition, prescribed burning produced similar magnitudes of effects compared to other factors. For wildfire scales, prescribed burning produced mostly nonsignificant effects, except for 2018 and 2019, where an increase in prescribed burning is connected to a decrease in wildfire scale. Prescribed burning also showed a delayed effect, where regions burned a year prior are subject to less severe wildfires the following year. In general, the effect of prescribed burning on wildfire scale is minimal compared to that of other factors such as precipitation. This is concerning since under the current scheme of climate change, weather conditions are expected to become more extreme, and if fire managers do not adapt their methods to the drastically changing climate, the effect of natural factors on wildfires would completely dominate that of prescribed burning.

KEYWORDS

non-linear model, mixed effect model, geographic information system, time series, CAL FIRE

INTRODUCTION

In the past decade, forest wildfires have become a prominent issue across the United States. Wildfire occurrences have increased in both overall frequency, severity, and area affected in all types of ecoregions at different rates (Dennison et al. 2014, Miller et al. 2020). The increase of fire activities is also disproportionately attributed to human activities versus natural phenomena, with human-caused fires accounting for 84% of all wildfires on government record from 1992 to 2012 (Balch et al. 2017). Wildfires have generated a $2 to $3 billion cost annually for governmental agencies, and the direct and indirect impact of wildfires are estimated at up to 30 times that cost (Schoennagel et al. 2016). More concerningly, human activities have expanded wildfire zones to regions that normally have low to moderate fire risks, introducing uncertainty to wildfire forecasts (Balch et al. 2017). And under this framework, wildfire prediction models now account for far more variability in residential wildfire risks than variations across climate scenarios that is originally considered the primary contributing factor to wildfires (Bryant and Westerling 2014). With these concerning components, agencies and managers are driven to develop fire management techniques to effectively and efficiently mitigate wildfires, with prescribed burning on one of the most important preemptive lines of defense (Forest Climate Action Team 2018).

In forest regions with high risk of wildfires, controlled burning of hazardous fuel, also known as prescribed burning, is often used to reduce the occurrences of large-scale natural fires (Vaillant et al. 2009). With detailed planning, forest and land managers aim to control the duration, frequency, and intensity of burning. Prescribed burning is effective in reducing the occurrence of large-scale wildfires, in both controlled experiments and computational simulations (Vaillant et al. 2009, Cassagne et al. 2011). Although controlled experiments are able to randomize treatment assignments and account for the stochastic nature of real forest ecosystems, their small scales relative to all forest regions limit the generalization of their results to larger scales (Fisher 1974, Vaillant et al. 2009). Simulations, on the other hand, are able to compute outcomes for a variety of natural system settings at a low cost, but are sometimes wanting in incorporating the complex interactions among natural components (Johnson et al. 2011, Moustakas and Davlias 2021). Moreover, both controlled experiments and simulations execute prescribed burning under idealized conditions and procedures that aim to optimize the outcome of the burning, which is

difficult to achieve in industrial practices (Fernandes and Botelho 2003, Vaillant et al. 2009, Cassagne et al. 2011).

The assumptions of how prescribed burning is conducted and the results of how prescribed burning affects the fire regime in both controlled experiments and simulations are difficult to achieve in large-scale practice. First, the researchers have control over the techniques used to conduct prescribed burning, as well as the approximate amount of fuel reduced (Vaillant et al. 2009, Cassagne et al. 2011), thus optimizing the decrease in fire severity. However, in reality, such optimum is rarely achieved. In California, the current regulation and permitting system regarding prescribed burning is largely inconsistent and suboptimal (Fernandes and Botelho 2003, Miller et al. 2020). As a result, despite fire management efforts, wildfire occurrences continue to increase in California (Dennison et al. 2014, Miller et al. 2020). Second, the results of controlled experiments and simulations cannot be easily generalized due to the spatial nonstationarity nature of wildfire trends. Wildfire trends of forest regions exhibit a non-uniform distribution across space (Li and Banerjee 2021), so the result from a controlled experiment that prescribed burning is effective in reducing wildfire in one area does not necessarily transfer to another area that has not been examined. Moreover, numerous factors contribute to wildfire trends, including climatic (e.g. temperature, precipitation), anthropic (e.g. distance of forests to roads or urban areas), geographical (e.g. elevation, slope), and fire management (e.g. frequency, intensity, and duration of prescribed burning) factors (North et al. 2012, D'Este et al. 2020, Moustakas and Davlias 2021). Particularly, climatic factors are undergoing drastic changes as a result of climate change, and such changes have significantly altered the fire regime in California (Williams et al. 2019). Thus understanding the effect of prescribed burning, confounded by time-dependent factors, requires analysis over an extended period of time, which controlled experiments, conducted over a short timeframe, cannot satisfy. A data-driven modeling approach, however, could mitigate the disadvantages of controlled experiment and simulations: It uses historic data of a large area (e.g. California) so that the result applies to all regions of the area; it can also incorporate the aforementioned factors and account for both spatial and temporal non-stationarity of wildfire trends.

This study models the importance of prescribed burning presence and scale as predictors of wildfire IDF under the current fire management approaches in California. I will identify covariates that contribute to wildfire trends and study the effect of 1) the presence of prescribed

burning on wildfire ignition probability and 2) the scale of prescribed burning on subsequent wildfire scales using a generalized additive model (GAM). I source data that serve as covariates from a collection of governmental and academic databases and combined into a comprehensive gridded geographic database. Observational studies on prescribed burning are relatively rare compared to other study designs, but drawing from existing studies (Balch et al. 2017, Moustakas and Davlias 2021), I hypothesize that out of the variety of climatic, geographic, and anthropic factors, the presence of prescribed burning will significantly reduce the chance that wildfires will occur, but the scale of prescribed burning will have little effect on wildfire scales, if a wildfire does occur.

METHODS

Study site

The study site is the State of California, where 33 million acres of forest area resides (California Department of Forestry and Fire Protection 2018). The California's Forests and Rangelands 2017 Assessment revealed that natural areas of California host over 7500 plant and animal species, with over 14 types of tree habitats (California Department of Forestry and Fire Protection 2018). There are over 15,000 protected areas owned and managed by federal, state, county, city, and private organizations (GreenInfo Network 2021). California also has a large population base of 39.5 million residents that are constantly reshaping the landscape of natural ecosystems. About 80 percent of the productive forest lands in California is for timber production, whose regulation varies from different types of ownership and management.

Data and metrics

To maximally capture wildfire trends, I included as many features as possible into my model and removed collinear features using the model selection process. Factors associated with change wildfire activities (Table 1) include temperature, precipitation, elevation, slope, population density, road distance, land cover type (D'Este et al. 2020), wind speed (Moustakas and Davlias 2021), land ownership (Miller et al. 2020), vapor pressure deficit (Zhuang et al.

Table 1. **Description of Data and Sources.** Data is downloaded from a variety of sources. For time-independent variables, the data from the most recent survey was acquired.

Feature Name	Description	Unit	Source	Citation
Prescribed burning data	Includes the start and end date, and intensity of fuel treatment	Varies	Department of Forestry and Fire Protection (CAL FIRE)	(CAL FIRE 2021a)
Wildfire data	Includes the ignition date and intensity of wildfire	Varies	USDA Forest Service	(Key and Benson 2005)
Temperature	Average annual temperature	°C	PRISM Climate Group	(PRISM Climate Group 2021)
Precipitation	Average annual precipitation	mm		
Vapor pressure deficit	Average annual vapor pressure deficit	haPa		
Population density	Number of residents in unit area	Persons per cell	US Census	(United States Census Bureau 2010)
Distance to closest road	Euclidean distance to the nearest road	km	US Geological Survey	(U.S. Geological Survey 2004)
Distance to hiking trail	Euclidean distance to the nearest hiking trail	km		(U.S. Geological Survey, National Geospatial Technical Operations Center 2021)
Elevation	Elevation above sea level	m		(U.S. Geological Survey 2021)
Slope	Slope	Degree		
Aspect	Sun-facing aspect	Degree		
Land coverage type	Proportion of type of vegetation coverage	Decimal proportion	Multi-Resolution Land Characteristics Consortium	(Dewitz 2021)
Wind speed	Average annual wind speed	m/s	National Renewable Energy Laboratory	(King et al. 2014, Draxl et al. 2015a, 2015b)
Cloud shading	Average annual cloud coverage	Decimal proportion	EarthEnv	(Torregrosa 2017)
Land ownership	Proportion of cell owned by each type of agency	Decimal Proportion	CAL FIRE	(CAL FIRE 2021b)
Distance to power line	Euclidean distance to electric transmission line	km	California Energy Commission	(California Energy Commission 2017)

2021), cloud shading (Williams et al. 2018), and fog frequency (Emery et al. 2018). For my data processing, I primarily used R with various packages (Gräler et al. 2016, Wood 2017, Fasiolo et al. 2018, Wickham et al. 2019, Arnold 2021, R Core Team 2021), and ArcGIS (Redlands 2011).

After obtaining these data, I constructed a geo-database that aggregates features into 4km by 4km grid cells. Data in each grid cell is calculated as an yearly average and averaged across the years of 2010 to 2019, as some data of 2020 has yet to be published. To reflect a general characteristic of each grid cell, I also averaged the yearly averages to obtain a single statistic (e.g. For temperature, each grid cell stores a yearly average from 2010 to 2019, and also an average temperature across all years). Lastly, to model the temporal differences in wildfire trends, I reshaped the data to a long format such that each data point represents a grid cell in a given year from 2010 to 2019.

To confirm these features' association with wildfire trends and motivate the use of a non-linear model, I computed the correlation coefficient (R^2) of each feature with the proportion of a grid cell that is burned in a year and generated pairplots of the features with wildfire proportion with a linear best-fit line.

The generalized additive model (GAM)

Model description

To assess the effect of prescribed burning and other factors on fire ignition probability and scale, I fitted a generalized additive model (GAM) over wildfire metrics on covariates. The general version of GAM can be described as

$$L(Y_c) = \alpha + \sum_{i=1}^{p} \quad f_i(X_{c,i}) + \epsilon_c, where\ \epsilon_c \sim N(0, \sigma^2),$$

where Y is the fire metrics, X the design matrix, L is the link function, p is the number of features used, c indexes each grid cell, and ϵ is the normally distributed error term with unknown variance (Hastie and Tibshirani 1999). Compared to a linear regression model, GAM does not assume linear relationship between the features and the response, so GAM does not fit a coefficient for each feature, rather, it fits a (not necessarily linear) smoothing function $f(\cdot)$ for each feature.

Furthermore, because some of the covariates are time-dependent, I used an extension of the GAM model, the generalized additive mixed-effects model (GAMM) so that data in each given year can be modeled separately (Pedersen et al. 2019). Generally, GAMM can be described as

$$L(Y_{c,y}) = \alpha + \sum_{i=1}^{p} f_{i,y}(X_{c,i}) + \epsilon_c, where\ \epsilon_c \sim N(0, \sigma^2)$$

Notice the additional index y that accounts for data in different years. Some covariates are time-independent so the same values are included when fitting $Y_{c,y}$ for a fixed c for all y; other time-dependent covariates would vary as y varies.

Model selection

GAM includes a family of models, so to fit a proper GAM over the data, I performed a systematic model selection process with the Akaike information criterion (AIC) as the criterion. First, a potential risk of GAM is overfitting, as the model fits very specific smoothing terms tailored to detailed trends in data (Zuur et al. 2009). To account for this, GAM allows manual selections of the dimension of the basis (the k parameter) for the smoothing term, as well as the amount of penalty applied for more complex smooths (the m parameter), both of which are reflected in the "wiggliness" of the fitted smoothing curve (Wood 2017). I used cross-validation to search for the best penalty term that minimizes AIC.

In addition, for the time-dependent variables, there are several choices to model their association with time. As Pedersen et al. (2019) outlined, I fitted 4 variants of the GAMM over the time-dependent variables: a global smoother for all observations (the G model), a global smoother with individual effects that have a shared penalty (the GS model), a global smoother with individual effects that have individual penalties (the GI model), and group-specific smoothers with a shared penalty and without a global smoother (the S model). I then compared the AIC computed for each model, selecting the one with the lowest AIC.

Model validation

After the optimal model was selected, I validated the model and checked for potential model misspecification. The main assumptions of the model include lack of concurvity,

appropriate conditional distribution of the covariates, and homoscedasticity. Concurvity is the nonlinear analogue to collinearity, and the presence of concurvity could affect the interpretability of model outcomes (Roy 2016). I computed the concurvity of each covariate and removed features that have a concurvity larger than 0.9. The distribution assumption of GAM is that given a vector of features, the outcomes are normally distributed (Zar 2010). This assumption is difficult to assess because the features are all continuous, so the joint probability of features equaling a set of values is theoretically zero. To approximate the distribution, I pooled the residuals of a fitted GAM and used a normal quantile-quantile plot to assess normality (Zuur et al. 2009). Because the sample size is large, I relaxed the normality assumption by allowing non-severe deviations from normality in the data (Faraway 2002, Zuur et al. 2009, Zar 2010). Lastly, to assess homoscedasticity, I first fitted GAM and computed the residuals. I plotted the residuals against the fitted values to look for patterns in the plot, and then plotted residuals against individual features to identify the sources of heteroskedasticity.

Modeling wildfire trends

Although I modeled both wildfire ignition probability and scale using GAM, different response types in these two models (binary vs. continuous) presented different modeling processes that will be discussed in this section.

Wildfire ignition probability

I defined wildfire ignition as whether there is at least one wildfire event in a grid cell in a given year. The binary nature of the response variable motivated me to use a logit link function for L, defined as

$$L(Y_{c,y}) = log(\frac{\pi_{c,y}}{1-\pi_{c,y}})$$

where $\pi_{c,y} = P(Y_{c,y} = 1)$ (Zuur et al. 2009). This particular link function requires care in the model validation and interpretation process. To test the homoscedastic assumption, I used an index plot instead of the usual fitted values vs. residuals plots, since the latter contains little information in the logistic setting (Pregibon 1981, Zuur et al. 2009). To interpret individual effects of the

smooths of each feature, I plotted the values of the feature against the inverse log-odds, which essentially demonstrated how much wildfire ignition probability that feature contributes to the overall probability.

Wildfire scale

The scale of wildfire is defined as the proportion of a grid cell that is burned in a year. Because the response is a proportion, I used the beta regression model. This mean that the link function is still the logit function, but now $\pi_{c,y}$ is the expectation of $Y_{c,y}$, which is assumed to follow a beta distribution (Ferrari and Cribari-Neto 2004). From there, I selected the model that minimizes AIC and tested the assumptions of the model as outlined in the model validation section. The interpretation of the smoothing terms in the Gaussian model was more straightforward than the logistic case, where the raw effect of each feature was plotted as how much it contributed to the overall response variable.

Feature importance

The feature importance of PB metrics relative to covariates illustrates how much prescribed burning contributes to wildfire metrics. Feature importance for nonlinear models (e.g. GAM) is more difficult to compare because with smoothing functions, there are no explicit coefficients to compare (Molnar 2021). Traditionally, the range of fitted values of the smoothing terms, as well as the p-value for each smoothing function could offer insights for how much each feature contributes to the outcome. A larger range and a smaller p-value would provide evidence that the feature contributes more to the outcome (Zuur et al. 2009). A more intuitive approach to nonlinear feature importance is the permutation feature importance (Molnar 2021). To obtain this metric, I shuffled the feature of interest and computed the root mean square error of the model. If a feature is more important, then shuffling that feature will produce a significantly larger error, and vice versa (Molnar 2021). I computed the three feature importance metrics described above and qualitatively compared the importance of each feature.

RESULTS

Model selection and validation

Among all models fitted, the GS model (global smoother and individual smoothers with shared penalty terms) obtained the least AIC. After the feature selection process, I removed nonsignificant features with p-values larger than 0.05. Both models on ignition probability and wildfire scale satisfied the normality assumption upon visual inspection. All features have concurvity less than 0.95 in both models. The residuals in both models did not appear to show significant patterns considering the fact that the range of values for both models are restricted (binary model {0,1} and continuous model [0,1]). I also conducted a validation search for the appropriate penalty term to prevent overfitting. The specifications and of the models were included in Appendix A and B.

Effect of factors on wildfire ignition

Using an absence-presence model on GAM, I studied the effect of different factors on fire ignition probability (Figure 1). Factors such as percentage of cell owned by a federal agency, distance to energy transmission line, and precipitation had a rather linear effect on fire ignition. For example, an increase from 50% to 60% in percentage of a cell owned by federal agency resulted in a increase of 0.15 in fitted log-odds (Figure 1c), whereas a unit increase in distance to energy transmission line (Figure 1d) resulted in a 8 percent decrease in ignition probability. Additionally, some factors exhibited more particular behavior. For instance, a relatively low (<5) or high (>20) temperature contributed significantly to a lower ignition probability, but at the intermediate range ([5,20]), temperature contributed little to ignition probability (Figure 1f). Similar trends were also observed in wind speed, slope, maximum vapor pressure deficit, deviation from mean temperature and precipitation, where ignition probability of regions with various factor values did not follow a linear relationship (Figure A2).

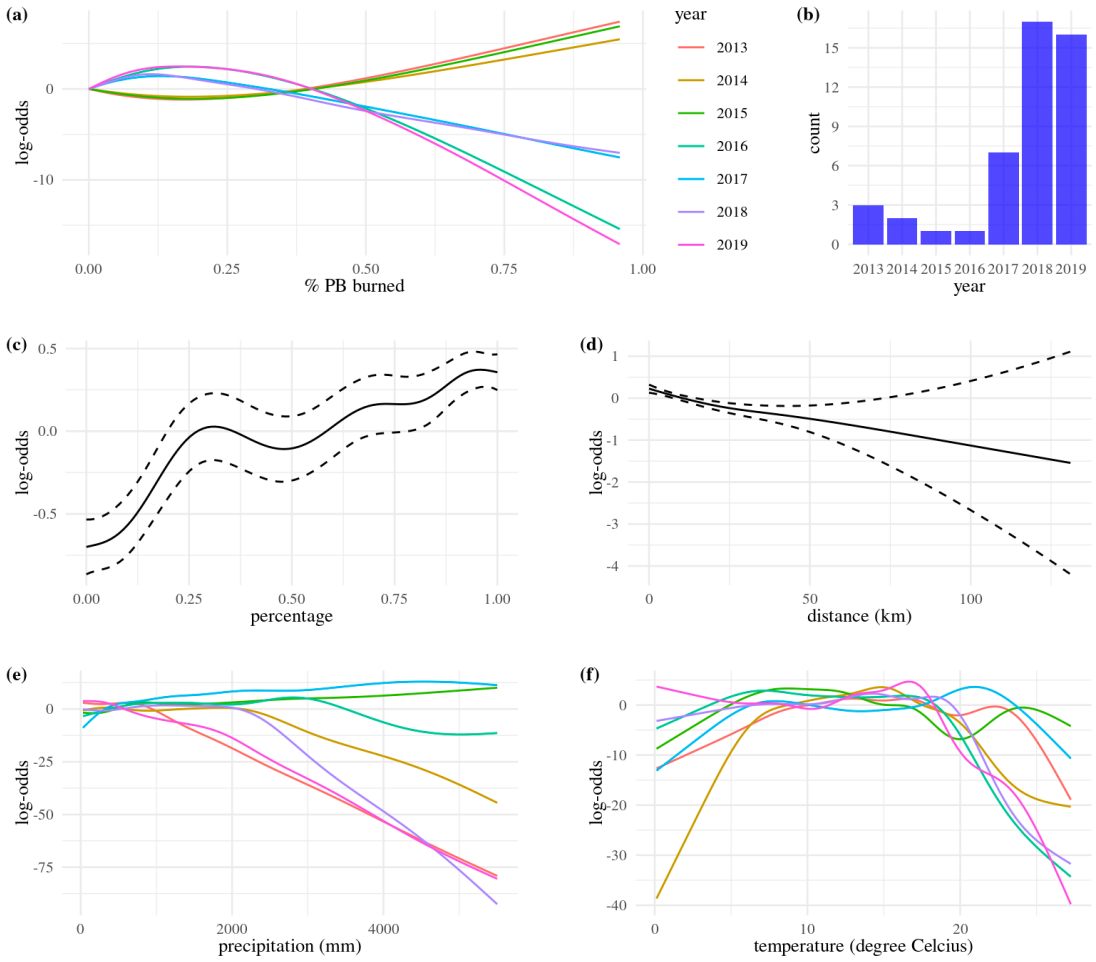

Figure 1. Fitted smooths of factors on wildfire ignition probability. Line plots of fitted log-odds of variables on wildfire ignition, with an additional auxiliary bar plot: (a) percentage of a cell treated by prescribed burning, (b) number of prescribed burning treatments with over 20% of grid cell area in each given year, (c) percentage of a grid cell owned by a federal agency, (d) distance of a cell to an energy transmission line, (e) mean annual precipitation, and (f) mean annual temperature. For year-dependent data, the lines are color-coded. For time-independent data, the solid line represents the mean estimate of the fitted smooth, and the dashed lines represent the boundaries of a 95% confidence interval for the fitted smooth.

Percentage of cell prescribed burns had a significant effect on wildfire ignition ($p < 2e\text{-}16$). Particularly, after 2016, the effect of prescribed burning was increasing from 0 to 0.2, then prescribed burning contributed decreasingly when the percentage increased from 0.2 (Figure 1a). During these years, a total of 6 large-scale prescribed burning (more than 20% grid burned) occurred (Figure 1b). The pattern was reversed in years before 2016 (Figure 1a), where a total of 39 large-scale prescribed burning was conducted (Figure 1b). In addition, the percentage prescribed burned several years prior to the year of interest also showed significant effects ($p =$

0.05 for 2 years prior; p = 0.002 for 3 years prior). Factors such as precipitation and temperature produced larger effects than prescribed burning (Figure 1e, f), while other factors such as federal land ownership and distance to energy transmission lines produced smaller effects (Figure 1c, d).

Effect of Factors on Wildfire Scale

Using the percentage burned in a grid cell as the dependent variable, I assessed the contribution of the prescribed burning percentage and other factors via GAM (Figure B2). Factors that showed linear relationships with wildfire scale, such as slope (Figure 2c) and deviation of mean annual precipitation (Figure 2e), overlap with those that showed linear relationships with fire ignition. Factors such as annual precipitation showed a nonlinear trend in relation to fire scale (Figure 2d). The effect of precipitation on the wildfire scale depended on the year of interest. In 2015 and 2017, increased precipitation is associated with larger wildfires, whereas in 2014 and 2018, wildfire scale decreased as more rainfall occurred (Figure 2d). Particularly, precipitation fluctuated with higher magnitude in 2018 than in 2015 (Figure 2f).

Prescribed burning score had a mostly nonsignificant relationship with fire score (p=0.99), except for 2016 and 2019 (Figure 2a). In 2016 and 2019 the relationship was non-linear, with fire scale increasing as prescribed burning percentage increased from 0 to 0.2; as prescribed burning percentage ranged from 0.2 and on, fire score decreased. However, in other years, the contribution of prescribed burning was practically zero. The effect of prescribed burning a year prior to the year when the wildfire occurred had similar magnitude as PB percentage during the current year, but with 4 years (2013-2014, 2018-2019) having more prominent effects than others (Figure 2b).

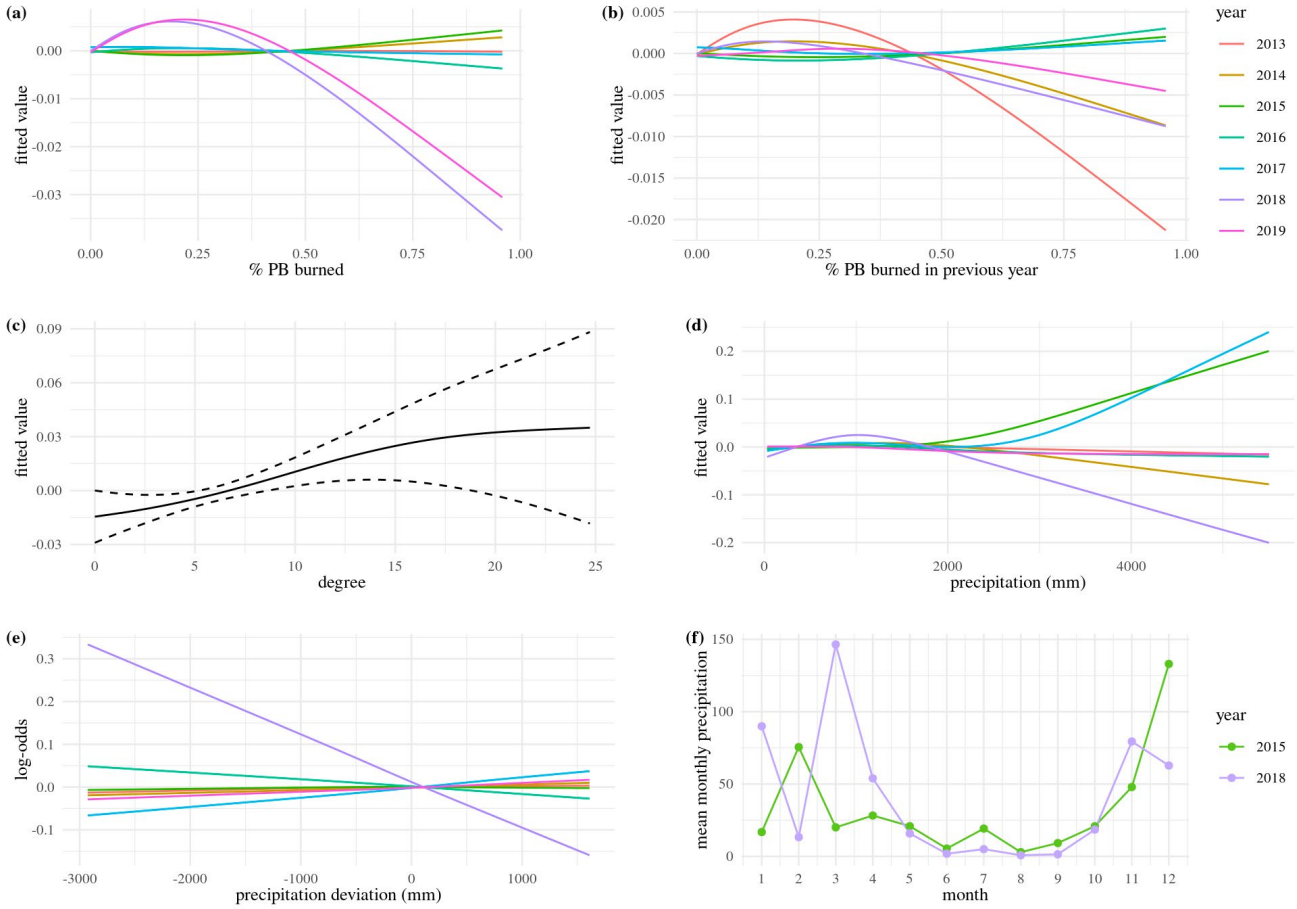

Figure 2. Fitted smooths of factors on wildfire scale. Line plots of fitted log-odds of variables on wildfire scale, with an additional auxiliary line plot: (a) percentage of a cell treated by prescribed burning during the year of interest, (b) percentage of a cell treated by prescribed burning during the year prior to the year of interest, (c) slope, (d) mean annual precipitation, (e) deviation of mean annual precipitation from the mean precipitation across all years studied, and (f) mean monthly precipitation in 2015 and 2018. For time-independent data, the solid line represents the mean estimate of the fitted smooth, and the dashed lines represent the boundaries of a 95% confidence interval for the fitted smooth.

DISCUSSION

Overall, prescribed burning is associated with decreased wildfire ignition probability, although the effect depends on various conditions in a given year. The effectiveness of prescribed burning and wildfire occurrences are significantly associated with weather conditions, such as temperature and precipitation, as well as human-related factors such as land ownership, and distance to energy transmission lines. Prescribed burning did not show a significant effect on wildfire scale; rather, other natural factors dominated the effect. With respect to wildfire scale,

mostly natural factors have the strongest influence, although extreme weathers on both ends of the spectrum produced varying effects depending on the time of the year these extreme conditions occurred.

Wildfire ignition probability

The fitted smooth for PB area demonstrates that in order for PB to effectively reduce wildfire occurrences, a sufficient level of burning is required. For recent years (2016-2019), a decrease in effect on wildfire ignition requires PB on approximately 20% of the area (Figure 1a). This is a significant area because each grid has an area of 25km^2, which is equivalent to 4600 standard football fields. With only 39 grids reaching this goal in 2018 and 2019 (Figure 1b), the current fire management plan in California proves to be suboptimal (Fernandes and Botelho 2003). In grids with prescribed burning percentage less than 20%, the positive fitted values can be a result of non-overlapping regions where PB and wildfires occurred separately. This phenomenon further enforces the argument that if a significant area within a grid is not treated, wildfires will emerge.

Furthermore, if only a small area is treated, the fire treatment will facilitate the regeneration process of local plantations (Simpson et al. 2019), and if the area occurs to be undergoing a dry season, the increased fuel load and reduced moisture content can further increase the chance a wildfire will occur (Kreye et al. 2013). In earlier years (2013-2015), the fitted smooth showed an increase with burned area. However, this estimate has a large uncertainty because there are only 6 large-scale (>20%) PB grids in these three years combined, and in 2014, no grid has received a PB percentage of greater than 50% (Figure 1b). Therefore, the positive effect shown on the smooth only reinforces the argument that the absence of large-scale PB events contribute to a slightly positive, although nonsignificant, wildfire ignition probability.

Aside from PB percentage, other factors also exhibited significant impacts on ignition probability. One of the most significant factors is mean annual temperature, with both low (<5 degrees Celsius) and high (>25 degrees Celsius) contributing a negative effect of magnitudes greater than 5 (Figure 1f). The effect of temperature on wildfires is a complex process dictated by how varying temperatures affect the accumulation of fuel that allows wildfires to occur. On the lower end, low temperature reduces vegetation growth, thus reducing the volume of potential fuels that facilitate wildfires (He et al. 2017). On the other hand, extremely high temperatures, in the

long run, can increase the rate of decomposition of debris from dead plants (Kennedy et al. 2021), thus reducing the amount of fuel available for wildfires to occur. Therefore, both low and high temperature can result in a decrease in wildfire activities, and as demonstrated by the effect size, variation in temperature has a larger effect than PB percentage, making temperature a more influential factor. Additionally, human-related factors also play a significant role in wildfire occurrences. The percentage of a grid owned by federal agencies had an increasingly positive effect on ignition probability (Figure 1c). This result largely corroborated with research that have attributed the increasing number of wildfires in California to mismanagement and long-term fire suppression from federal fire managers (Starrs et al. 2018). Therefore, the cautionary tale of increasing wildfire occurrences associated with federal land ownership calls for attention for federal agencies to take actions and improve their fire management efforts.

Wildfire scale

In relation to the percentage of a cell burned by wildfires, PB percentage did not reveal a significant effect across years. Although overall, the effect of PB has an extremely large p-value ($p=0.99$), the fitted smooth of 2018 and 2019 still revealed valuable information. The largest effects of these two years are about -0.03 (Figure 2a), meaning that maximum PB effort can reduce the percentage of wildfire burned by 3%, equivalent to an area of $0.75km^2$ (138 standard football fields). In practical terms, this is still a very significant area, despite the overall effect being nonsignificant compared to the size of grid cells. In these two years, the fitted values of PB percentage showed a similar trend to that on ignition probability, where only burning an adequate amount can have a significant reduction effect on wildfire scale. Although PB conducted during the year when wildfires occur did not have a significant impact on wildfire scale, in several years (2013-2014, 2018-2019), PB conducted in the year prior to wildfire ignition showed a delayed effect that reduced wildfire scales in the following year (Figure 2b). PB alters the structures of forest ecosystems, reducing surface coverage and raising canopies, but this process requires time even after burning is conducted (Elliott et al. 2009), resulting in an nonsignificant effect of burning during the year of wildfires, as well as a delayed effect of PB.

In terms of contribution to the wildfire scale, natural factors seemed to dominate. The most significant factor is average annual precipitation, with a maximum effect of magnitude 0.2 (Figure

2d). However, several years showed contrasting results. In 2015 and 2016, increasing precipitation results in increased wildfire scales, whereas in 2014 and 2018, an increase in precipitation was associated with decreased wildfire scale. This phenomenon is related to the intra-year pattern of precipitation (Figure 2f). For example, in 2015, higher precipitation events happened in February, facilitating plant growth, thus increasing the amount of biomass for fires to consume (Nafus et al. 2017). On the other hand, in 2018, although the precipitation was high early in the year, the high precipitation continued leading up to the fire season, increasing moisture content in the plant and soil (Wang et al. 2019), decreasing wildfire risk (Krueger et al. 2015). In addition, extreme precipitation conditions, quantified by the deviation of rainfall from the overall average, showed a similar magnitude of effects on wildfire scale (Figure 2e). This further enforces the idea that the effect of natural factors on wildfire scale varies depending on specific conditions in specific years. Compared to PB percentage, this natural factor has a much larger influence on wildfire scales.

Conclusion

Overall, prescribed burning produces a significant effect on reducing both the ignition probability and scale of wildfires. Compared to prescribed burning's effect on the chance of wildfire ignitions, PB's effect on wildfire scales is lower in magnitudes and dominated by the effect of natural factors. Both effects showed significant correlation to time, where the effect at reducing wildfires vary across the years studied. The main factor that dictates how effective prescribed burning is relies on an adequate area burned within each grid, where a burn less than ~20% is essentially nonsignificant. Analysis on natural factors showed that the effect of PB on reducing wildfires is highly dependent on weather conditions and the specific environments of the area burned. Lastly, in both ignition probability and scale, PB revealed a delayed effect where several years' of burning accumulated and produced a synergistic effect years later.

Limitations

Firstly, the temporal resolution of data is year, and as demonstrated by the data, within-year variations of the factors can reveal significant insights. For example, factors such as precipitation tends to vary throughout a year, and the variation can have different effects on

vegetation during different seasons (Yan et al. 2015). This study did not include seasonal data mainly due to constraints on computing power, as the current model takes 30 minutes to one hour to run each cycle. Therefore, more computing power would allow the analysis to examine the effects on a finer scale, and thus produce a more insightful result.

Secondly, this study only included data from 2013 to 2019, although data from 2010 to 2012 were included implicitly to compute lagged variables on PB conducted in these years. As wildfires have been increasing in the recent decade, I decided to only include the last decade to examine the most severe wildfires. However, climate patterns seem to fluctuate across years (Vincze et al. 2017); with this high variability, including data on more years could incorporate a more diverse range of weather conditions into the model and allows examination of wildfire behavior under these conditions.

Broader implications

The study demonstrates that natural and human-related factors often have a stronger effect on both wildfire ignition probability and wildfire scale, although the delta is higher for the latter. Under the current scheme of climate change, occurrences of extreme weather events are becoming more frequent (Williams et al. 2019). If natural factors take on more extreme values, their effect on wildfires could essentially dominate the effects of PB and make PB's effect completely nonsignificant. Meanwhile, current fire management plans have been static and unresponsive to the drastically changing climate (Calkin et al. 2015, Kolden 2019). Therefore, it is imperative that fire managers examine the weather conditions and treat vegetation fuels and wildfires in a way that accounts for these weather conditions. This study has demonstrated that prescribed burning, when done adequately and appropriately, can be effective, so with proper management, it is possible that wildfires can be properly prevented and reduced.

ACKNOWLEDGEMENTS

I would like to express my gratitude for the ESPM 175 teaching team, especially Dr. Patina Mendez, for your patience, encouragement, and timely feedback. The conception of my study is inspired by my previous works done with Dr. Polly Buotte, my mentor, who has always supported

me through her expertise in forest ecology and wildfires. I am so honored to have her as my mentor. I would also like to thank my friends, Brandon, Ashwin, Saira, Marcus, Keren, Cade, Amit, and Ariana, who always encouraged me throughout the project. Lastly, to my family, thank you for everything you have done to support my education.

REFERENCES

Arnold, J. B. 2021. ggthemes: Extra Themes, Scales and Geoms for "ggplot2."

Balch, J. K., B. A. Bradley, J. T. Abatzoglou, R. C. Nagy, E. J. Fusco, and A. L. Mahood. 2017. Human-started wildfires expand the fire niche across the United States. Proceedings of the National Academy of Sciences of the United States of America 114:2946–2951.

Bryant, B. P., and A. L. Westerling. 2014. Scenarios for future wildfire risk in California: links between changing demography, land use, climate, and wildfire. Environmetrics 25:454–471.

CAL FIRE. 2021a, April 16. Prescribed Fire Burns - California [ds397].

CAL FIRE. 2021b, July 30. California Land Ownership.

California Department of Forestry and Fire Protection. 2018. California's Forests and Rangelands 2017 Assessment:318.

California Energy Commission. 2017, December 27. California Electric Transmission Lines.

Calkin, D. E., M. P. Thompson, and M. A. Finney. 2015. Negative consequences of positive feedbacks in US wildfire management. Forest Ecosystems 2:9.

Cassagne, N., F. Pimont, J.-L. Dupuy, R. R. Linn, A. Mårell, C. Oliveri, and E. Rigolot. 2011. Using a fire propagation model to assess the efficiency of prescribed burning in reducing the fire hazard. Ecological Modelling 222:1502–1514.

Dennison, P. E., S. C. Brewer, J. D. Arnold, and M. A. Moritz. 2014. Large wildfire trends in the western United States, 1984–2011. Geophysical Research Letters 41:2928–2933.

D'Este, M., A. Ganga, M. Elia, R. Lovreglio, V. Giannico, G. Spano, G. Colangelo, R. Lafortezza, and G. Sanesi. 2020. Modeling fire ignition probability and frequency using Hurdle models: a cross-regional study in Southern Europe. Ecological Processes 9:N.PAG-N.PAG.

Dewitz, J. 2021, June 4. National Land Cover Database (NLCD) Land Cover Change Index Conterminous United States. U.S. Geological Survey.

Draxl, C., B. M. Hodge, A. Clifton, and J. McCaa. 2015a. Overview and Meteorological Validation of the Wind Integration National Dataset Toolkit (Technical Report,

NREL/TP-5000-61740). National Renewable Energy Laboratory, Golden, CO.

Draxl, C., B. M. Hodge, A. Clifton, and J. McCaa. 2015b. The Wind Integration National Dataset (WIND) Toolkit. Applied Energy 151:6.

Elliott, K. J., J. M. Vose, and R. L. Hendrick. 2009. Long-Term Effects of High Intensity Prescribed Fire on Vegetation Dynamics in the Wine Spring Creek Watershed, Western North Carolina, USA. Fire Ecology 5:66–85.

Emery, N. C., C. M. D'Antonio, and C. J. Still. 2018. Fog and live fuel moisture in coastal California shrublands. Ecosphere 9:e02167.

Faraway, J. J. 2002. Practical Regression and Anova using R:213.

Fasiolo, M., R. Nedellec, Y. Goude, and S. N. Wood. 2018. Scalable visualisation methods for modern Generalized Additive Models. Arxiv preprint.

Fernandes, P. M., and H. S. Botelho. 2003. A review of prescribed burning effectiveness in fire hazard reduction. International Journal of Wildland Fire 12:117.

Ferrari, S., and F. Cribari-Neto. 2004. Beta Regression for Modelling Rates and Proportions. Journal of Applied Statistics 31:799.

Fisher, R. A. 1974. The design of experiments. Hafner Press, New York.

Forest Climate Action Team. 2018. California Forest Carbon Plan: Managing Our Forest Landscapes in a Changing Climate:186.

Gräler, B., E. Pebesma, and G. Heuvelink. 2016. Spatio-Temporal Interpolation using gstat. The R Journal 8:204–218.

GreenInfo Network. 2021, July. CPAD Database Manual.

Hastie, T., and R. Tibshirani. 1999. Generalized additive models. Chapman & Hall/CRC, Boca Raton, Fla.

He, B., A. Chen, W. Jiang, and Z. Chen. 2017. The response of vegetation growth to shifts in trend of temperature in China. Journal of Geographical Sciences 27:801–816.

Johnson, M. C., M. C. Kennedy, and D. L. Peterson. 2011. Simulating fuel treatment effects in dry forests of the Western United States: testing the principles of a fire-safe forest.(Report). Canadian Journal of Forest Research 41:1018.

Kennedy, M. C., R. R. Bart, C. L. Tague, and J. S. Choate. 2021. Does hot and dry equal more wildfire? Contrasting short- and long-term climate effects on fire in the Sierra Nevada, CA. Ecosphere 12.

Key, C. H., and N. C. Benson. 2005. Landscape Assessment (LA):55.

King, J., A. Clifton, and B. M. Hodge. 2014. Validation of Power Output for the WIND Toolkit (Technical Report, NREL/TP-5D00-61714). National Renewable Energy Laboratory,

Golden, CO.

Kolden, C. A. 2019. We're Not Doing Enough Prescribed Fire in the Western United States to Mitigate Wildfire Risk. Fire 2:30.

Kreye, J. K., L. N. Kobziar, and W. C. Zipperer. 2013. Effects of fuel load and moisture content on fire behaviour and heating in masticated litter-dominated fuels. International Journal of Wildland Fire 22:440–445.

Krueger, E. S., T. E. Ochsner, D. M. Engle, J. D. Carlson, D. Twidwell, and S. D. Fuhlendorf. 2015. Soil Moisture Affects Growing-Season Wildfire Size in the Southern Great Plains. Soil Science Society of America Journal 79:1567–1576.

Li, S., and T. Banerjee. 2021. Spatial and temporal pattern of wildfires in California from 2000 to 2019. Scientific Reports 11:8779.

Miller, R. K., C. B. Field, and K. J. Mach. 2020. Barriers and enablers for prescribed burns for wildfire management in California. Nature Sustainability 3:101–109.

Molnar, C. 2021. Interpretable Machine Learning.

Moustakas, A., and O. Davlias. 2021. Minimal effect of prescribed burning on fire spread rate and intensity in savanna ecosystems. Stochastic Environmental Research and Risk Assessment 35:849–860.

Nafus, M. G., T. D. Tuberville, K. A. Buhlmann, and B. D. Todd. 2017. Precipitation quantity and timing affect native plant production and growth of a key herbivore, the desert tortoise, in the Mojave Desert. Climate Change Responses 4:4.

North, M., B. M. Collins, and S. Stephens. 2012. Using Fire to Increase the Scale, Benefits, and Future Maintenance of Fuels Treatments. Journal of Forestry 110:392–401.

Pedersen, E. J., D. L. Miller, G. L. Simpson, and N. Ross. 2019. Hierarchical generalized additive models in ecology: an introduction with mgcv. PeerJ 7:e6876.

Pregibon, D. 1981. Logistic Regression Diagnostics. The Annals of Statistics 9:705–724.

PRISM Climate Group. 2021, November 14. Climate Data. Oregon State University.

R Core Team. 2021. R: A Language and Environment for Statistical Computing. R Foundation for Statistical Computing, Vienna, Austria.

Redlands, C. E. S. R. I. 2011. ArcGIS Desktop: Release 10.

Roy, J. 2016, September 26. GAMs, Part II: https://jroy042.github.io/nonlinear/week3.html.

Schoennagel, T., P. Morgan, J. Balch, P. Dennison, B. Harvey, M. Krawchuk, M. Moritz, R. Rasker, and C. Whitlock. 2016. Insights from wildfire science: A resource for fire policy discussions:9.

Simpson, K. J., J. K. Olofsson, B. S. Ripley, and C. P. Osborne. 2019. Frequent fires prime plant

developmental responses to burning. Proceedings of the Royal Society B: Biological Sciences 286:20191315.

Starrs, C. F., V. Butsic, C. Stephens, and W. Stewart. 2018. The impact of land ownership, firefighting, and reserve status on fire probability in California. Environmental Research Letters 13:034025.

Torregrosa, A. 2017, November 2. Decadal Fog and Low Cloud Frequency Spatial Dataset. California Landscape Conservation Cooperative.

United States Census Bureau. 2010. California Population Density. United States Census Bureau.

U.S. Geological Survey. 2004. National Overview Road Metrics - Euclidean Diance (NORM-ED) Lower 48 States. U.S. Geological Survey, Denver, CO.

U.S. Geological Survey. 2021, November 1. USGS 1 arc-second 1 x 1 degree. U.S. Geological Survey.

U.S. Geological Survey, National Geospatial Technical Operations Center. 2021, November 15. USGS National Transportation Dataset (NTD) for California 20211115 State or Territory Shapefile: U.S. Geological Survey.

Vaillant, N. M., J. A. Fites-Kaufman, and S. L. Stephens. 2009. Effectiveness of prescribed fire as a fuel treatment in Californian coniferous forests. International Journal of Wildland Fire 18:165.

Vincze, M., I. D. Borcia, and U. Harlander. 2017. Temperature fluctuations in a changing climate: an ensemble-based experimental approach. Scientific Reports 7:254.

Wang, Y., J. Yang, Y. Chen, G. Fang, W. Duan, Y. Li, and P. De Maeyer. 2019. Quantifying the Effects of Climate and Vegetation on Soil Moisture in an Arid Area, China. Water 11:767.

Wickham, H., M. Averick, J. Bryan, W. Chang, L. D. McGowan, R. François, G. Grolemund, A. Hayes, L. Henry, J. Hester, M. Kuhn, T. L. Pedersen, E. Miller, S. M. Bache, K. Müller, J. Ooms, D. Robinson, D. P. Seidel, V. Spinu, K. Takahashi, D. Vaughan, C. Wilke, K. Woo, and H. Yutani. 2019. Welcome to the tidyverse. Journal of Open Source Software 4:1686.

Williams, A. P., J. T. Abatzoglou, A. Gershunov, J. Guzman-Morales, D. A. Bishop, J. K. Balch, and D. P. Lettenmaier. 2019. Observed Impacts of Anthropogenic Climate Change on Wildfire in California. Earth's Future 7:892–910.

Williams, A. P., P. Gentine, M. A. Moritz, D. A. Roberts, and J. T. Abatzoglou. 2018. Effect of Reduced Summer Cloud Shading on Evaporative Demand and Wildfire in Coastal Southern California. Geophysical Research Letters 45:5653–5662.

Wood, S. N. 2017. Generalized additive models: an introduction with R. Second edition. CRC Press/Taylor & Francis Group, Boca Raton.

Yan, H., C. Liang, Z. Li, Z. Liu, B. Miao, C. He, and L. Sheng. 2015. Impact of Precipitation Patterns on Biomass and Species Richness of Annuals in a Dry Steppe. PLOS ONE 10:e0125300.

Zar, J. H. 2010. Biostatistical analysis. 5th ed. Prentice-Hall/Pearson, Upper Saddle River, N.J.

Zhuang, Y., R. Fu, B. D. Santer, R. E. Dickinson, and A. Hall. 2021. Quantifying contributions of natural variability and anthropogenic forcings on increased fire weather risk over the western United States. Proceedings of the National Academy of Sciences 118.

Zuur, A. F., Elena N. Ieno, Neil J. Walker, Anatoly A. Saveliev, and Graham M. Smith. 2009. Mixed effects models and extensions in ecology with R. Springer, New York, NY.

APPENDIX A: Model specification and outputs for ignition probability

Table A1. Model specification for the binary model. All terms are run with a smooth, with factors that do not have random effects using the default "tp" basis, and random effect factors using the "fs" basis. The model is run with a binomial family, with the parameter "select" set to true. D means that the variable is related to a distance, and D* refers to deviation from the overall mean across the years.

Label	Variable	Random Effect
(a)	Precipitation	year
(b)	D* precipitation	year
(c)	Temperature	year
(d)	D* temperature	year
(e)	Max VPD	year
(f)	D* Max VPD	year
(g)	Cloud coverage	none
(h)	Wind Speed	none
(i)	Herb coverage	none
(j)	Elevation	none
(k)	Slope	none
(l)	Federal ownership	none
(m)	State ownership	none
(n)	D hiking trail	none
(o)	D power line	none
(p)	percentage prescribed burned	year
(q)	percentage prescribed burned (1 year prior)	year
(r)	percentage prescribed burned (2 years prior)	year
(s)	percentage prescribed burned (3 years prior)	year
	Coordinates (x and y)	year

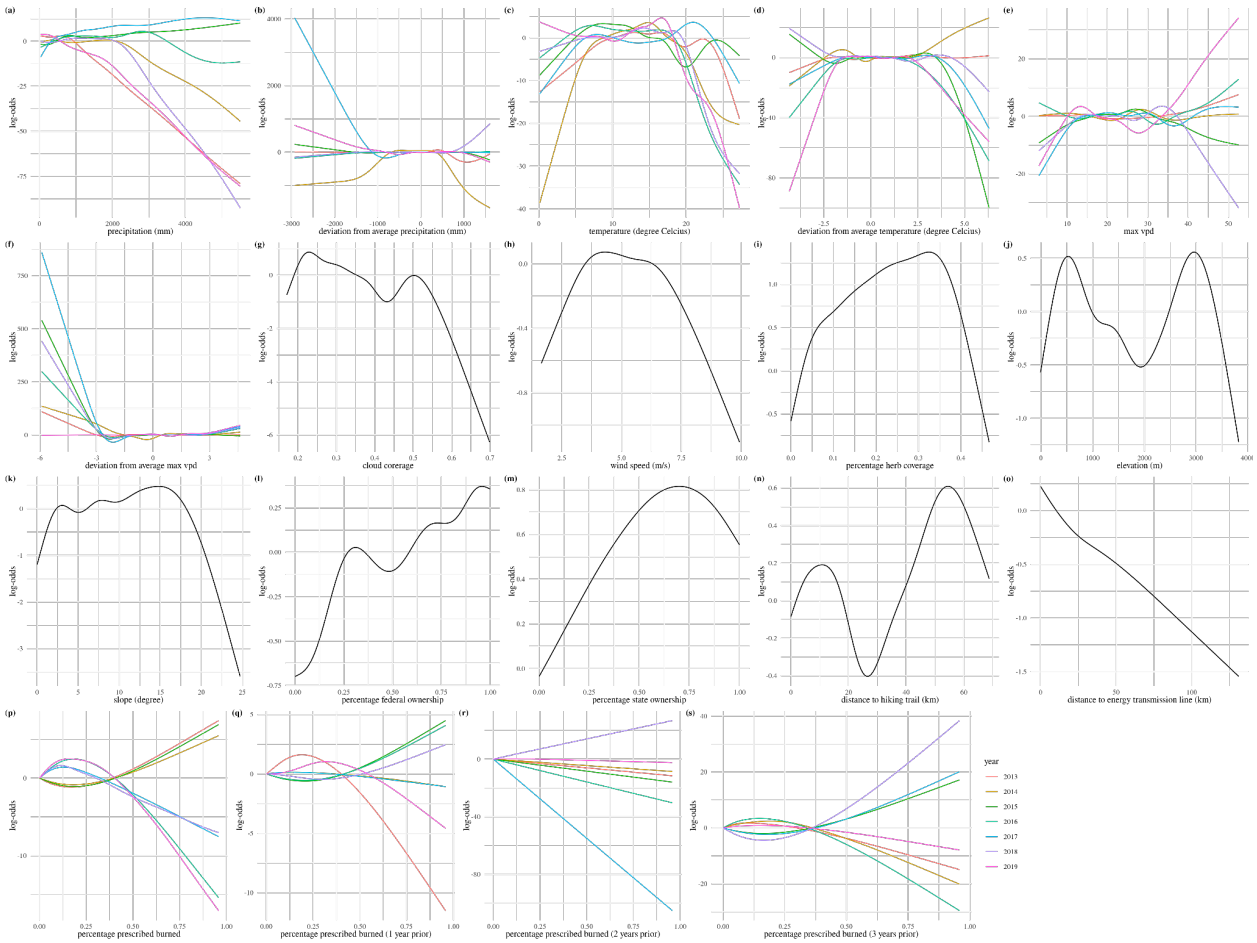

Figure A1. Model output for the binary model. For year-dependent data, the lines are color-coded. The letter labels correspond to the variables in Table A1.

APPENDIX B: Model specification and outputs for wildfire scale

Table B1. Model specification for the continuous model. All terms are run with a smooth, with factors that do not have random effects using the default "tp" basis, and random effect factors using the "fs" basis. The model is run with a betar family, with the parameter "select" set to true. D means that the variable is related to a distance, and D* refers to deviation from the overall mean across the years.

Label	Variable	Random Effect
(a)	Precipitation	year
(b)	D* precipitation	year
(c)	Temperature	year
(d)	D* temperature	year
(e)	Max VPD	year
(f)	D* Max VPD	year
(g)	Cloud coverage	none
(h)	Herb coverage	none
(i)	Elevation	none
(j)	Slope	none
(k)	Population density	none
(l)	Federal ownership	none
(m)	State ownership	none
(n)	percentage prescribed burned	year
(o)	percentage prescribed burned (1 year prior)	year
(p)	percentage prescribed burned (2 years prior)	year
(q)	percentage prescribed burned (3 years prior)	year
	Coordinates (x and y)	year

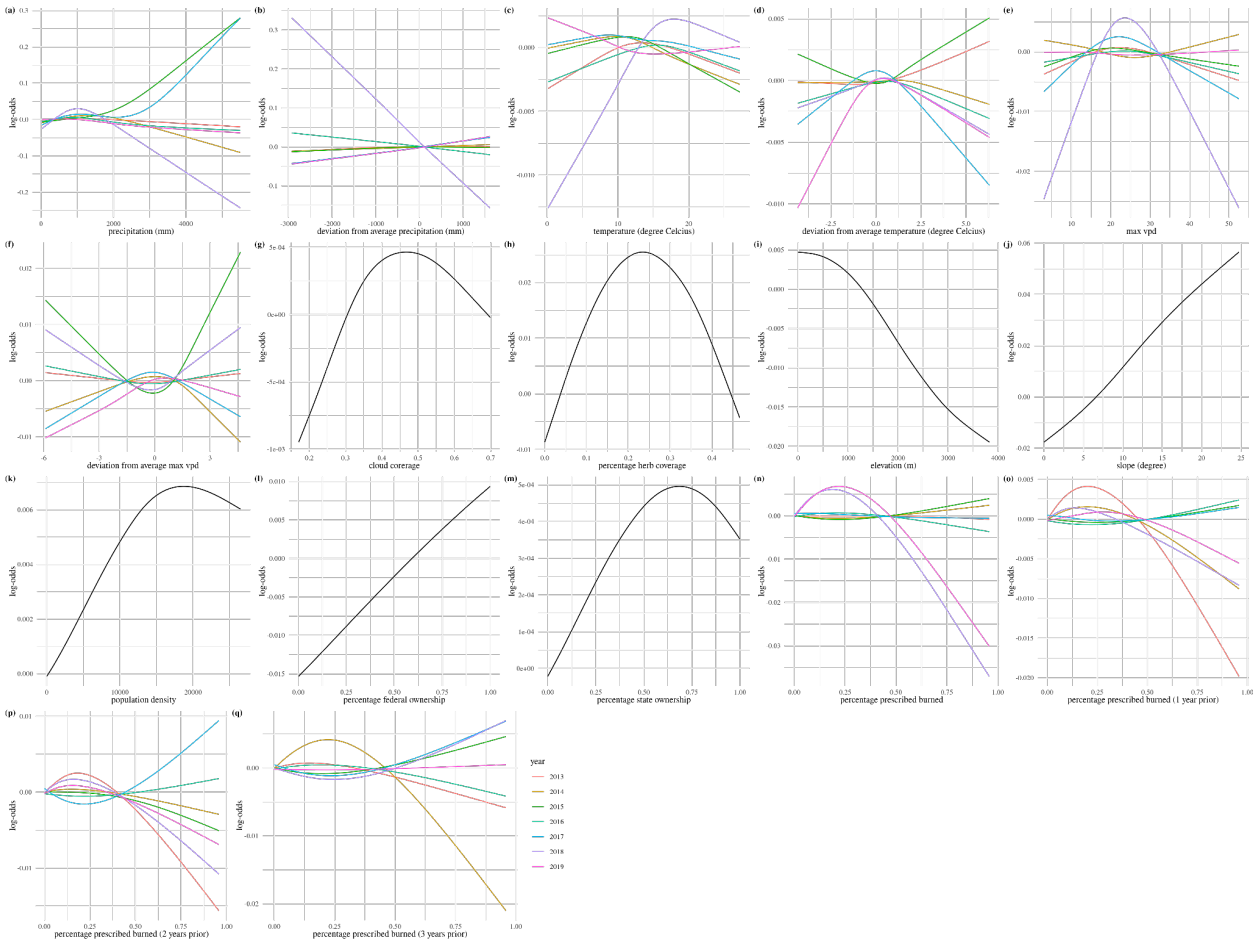

Figure B1. Model output for the continuous model. For year-dependent data, the lines are color-coded. The letter labels correspond to the variables in Table B1.